Quételet's fringes due to scattering by small spheres just above a reflecting surface

Wilfried Suhr* and H. Joachim Schlichting

University of Münster, Institut für Didaktik der Physik, Wilhelm-Klemm-Strasse 10, 48149 Münster, Germany

*Corresponding author: wilfried.suhr@uni-muenster.de

Received 6 May 2009; revised 19 August 2009; accepted 21 August 2009;
posted 24 August 2009 (Doc. ID 110998); published 2 September 2009

In various everyday situations, a characteristic interference pattern can be observed on water surfaces. This pattern can be divided into two overlapping components: a corona and a system of Quételet's rings, often with only a section of these visible in the form of fringes. We attribute this phenomenon to thin films of small spheres located just above the reflecting water surface. Due to differences in the optical arrangement, explanatory models applicable for conventionally produced Quételet's rings are not transferable. We present a compatible mathematical model and some obvious analogies in order to explain the occurrence and properties of this phenomenon. © 2009 Optical Society of America

OCIS codes: 290.5850, 260.3160.

1. Introduction

A natural optical phenomenon occurs sporadically on ponds and pools during warm seasons when a system of concentric colored rings superposed with a system of horizontal fringes appears around the image of the Sun on the surface of the water (Fig. 1). The first publication to interpret these horizontal fringes as a section of Quételet's rings was written by one of us [1], indicating that the Quételet's rings are not just a laboratory phenomenon but can be observed in nature as well. The first documented observations of a class of corresponding phenomena can be found in Newton's *Opticks* [2], where he called them "Colours of thick transparent polish'd Plates," nowadays better known as Quételet's rings. Newton's "dusty mirror" experiment is still the best-known method to produce these. For this, a backsilvered mirror whose glass surface holds scattering particles, such as dust, is used. When the mirror is illuminated from a point not far from the axis of the mirror and the reflection of the light source is observed, a system of concentric colored rings becomes recognizable. There are two typical characteristics of such Quételet's rings: the position of the reflection of the light source is eccentric and, in addition, the sequence of rings of same color is symmetrical on both sides of the achromatic ring that passes through the reflection of the light source. Examples of alternative methods for the production of Quételet's rings are described in [3,4]. Stokes has presented a general theory for this phenomenon [5], according to which it results from interference between two streams of light, one scattered upon entering the glass and the other scattered on emerging from the glass. A summary of this theory can be found in [6].

During qualitative investigation of the above mentioned interference pattern on ponds and pools, we discovered the solid angle covering this pattern to be independent from the distance to the observer, demonstrating that the zone visible around the pattern expands when the observer's eye approaches the surface of the water. With an increasing field of view, the apparently horizontal fringes emerged as a sector of a much larger second system of concentric colored rings (Fig. 2). The position of the reflection of the Sun was eccentric to these rings. As stated above, this eccentricity is a characteristic of Quételet's rings. Symmetry on both sides of the achromatic ring passing through the reflection of the Sun was also observed in the sequence of same-colored rings on the fringes, giving further proof for the assumption that these were Quételet's rings.

0003-6935/09/264978-07$15.00/0
© 2009 Optical Society of America

Fig. 1. (Color online) Algal film on the surface of the water causes the interference pattern surrounding the reflection of the Sun.

Although color patterns on ponds have been observed by many people, we could find no reference to an interpretation of them as Quételet's rings before publication by one of us, indicating that the appearance of Quételet's rings on the surface of a liquid seems to be a new finding. In reference to classical experiments, we first assumed that the surface of the water would be covered by a transparent layer bearing particles of dust on top. However, annotations from other scientists as well as our own microscopic investigations convinced us that this film resulted from an accumulation of single-celled algae on the water surface. At that time, our attempts to develop a model explaining the formation of Quételet's rings in such algal films failed because we knew too little about their structure.

2. Insights through Looking at Hot Tea

Another phenomenon that did not seem to be associated with Quételet's rings on ponds helped to solve this problem. If the surface of a hot drink, tea or black coffee, for example, is illuminated, shimmering colors can be observed around the reflection of the light source. A qualitative description of this phenomenon was given by Schaefer in 1971 [7]. Accordingly, the shimmering colors can be interpreted as a corona caused by forward scattering on lots of tiny water droplets almost equal in size and floating as a thin layer just above the surface of the water. These droplets are levitated by an intense flux of water vapor. Since droplets that are too large fall back into the liquid and those too small drift away up into the air, only droplets of a particular size are held in hovering flight. Single droplets hovering in the flimsy layer on the surface of the water can be recognized through a magnifying glass (Fig. 3).

Our investigations revealed that a corona appears not only on tea or coffee but also on the surface of pure hot water. For this purpose, the water must have a low level of hardness and a temperature between 60 °C and 80 °C. Light from an extended light source (the Sun, for example) that has passed through a circular aperture is suitable for illumination. The light cone projected should fall onto the surface of the water at a flat angle of incidence. When a cup is filled to the brim with hot water and viewed with good illumination, a corona surrounding the reflection of the light source can be recognized. The size of the visible section of the corona depends on the observation distance. From a distance of about 50 cm, the section cut out by the brim appears as an expanded color pattern with smooth transitions. To obtain a wide angle view capturing the whole corona within the cup, the distance between the observer and the surface of the water has to be reduced to a few centimeters. A focus close to the surface of the water makes the corona appear blurry. This is due to the fact that the image of the light source is beyond the depth of field. In accordance with a blurred optical image of the light source, the diffraction pattern produced is also blurred. We were surprised at what happened when we shifted the focus to the image of the light source. In addition to the corona, whose curves then looked perfect, horizontal fringes superimposing the system of rings emerged (Fig. 4, bottom). Up to now, there have been no reports of these. These fringes also possess the characteristics of Quételet's fringes, as described above, and, accordingly, have to be considered as a section of Quételet's

Fig. 2. (Color online) View from a short distance of an interference pattern caused by an algal film on a sample of water from the pond shown in Fig. 1. Slightly bent Quételet's fringes overlap a corona that surrounds the reflection of the artificial light source.

Fig. 3. (Color online) Close-up image of a thin layer of water droplets that are levitated by the flux of water vapor from the surface of hot water (~70 °C).

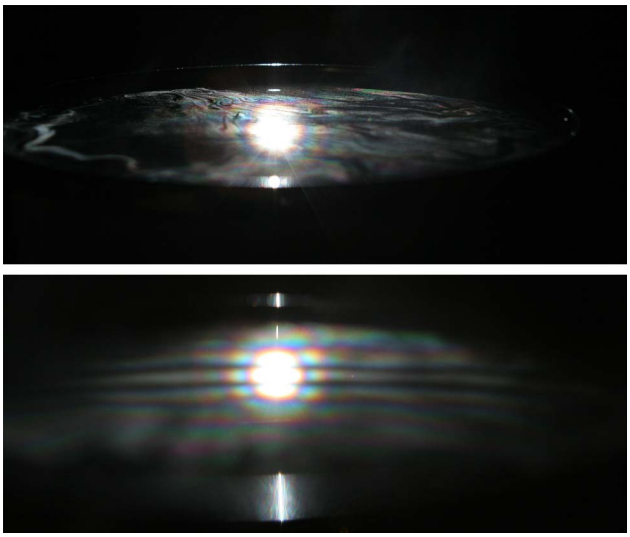

Fig. 4. (Color online) Top: focusing on the layer of droplets on the water surface makes the corona appear blurry. Bottom: if, instead, the focus is shifted to the image of the light source, a more pronounced corona as well as, horizontal fringes emerge.

rings whose diameter, depending upon the angle of incidence of the light, can become quite large in comparison to the diameter of the visible rings of the corona.

Altogether, we now knew two kinds of water-covering layers that contribute to the formation of Quételet's fringes. Since the respective phenomena resemble one another qualitatively, it could be assumed in both cases that there are great similarities in their optical constellation. In the case of hot water, only a magnifying glass was necessary to recognize that the layer floating on the mirroring water surface consisted of tiny droplets. As the algal film on the pond also consists of tiny spheres, the similarity between both phenomena became apparent. In the master thesis of Riikonen [8] we found that almost spherical algae are carried by a short stem above the surface of the water, so that we have almost the same physical situation. In accordance with our findings about the water droplets hovering on the surface of hot tea Riikonen recognized full emergence of the algae as a prerequisite for formation of Quételet's fringes. Riikonen's thesis is one of the most extensive works on the formation of coronas, glories, and Quételet's rings due to algal films. Its many excellent images were very helpful in our deliberations.

In the case of hot water as well as that of algal films, the elementary constellation of a small sphere close to a mirroring surface is found. An accumulation of small spheres forms a flat layer with mostly free space between neighboring spheres. On the basis of this concept, we developed a theoretical model in order to open quantitative access to the described phenomena.

3. Model Representations

In order to get a satisfying physical explanation of the optical phenomena described above, a numerical simulation model was developed. It is based on a strongly idealized version that first considers only those optical processes that contribute exclusively to the formation of Quételet's fringes.

For simplification, we assume a planar layer consisting of uniform spheres distributed spatially at random. This layer is a plane parallel to a mirroring surface and levitates a short distance above it. A planar harmonic wave is used to illuminate the layer. Since secondary illumination by scattering or reflection on neighboring spheres is neglected, we can assume that all the spheres are illuminated in a similar manner and that, therefore, all of them undergo the same optical process. To check in a practical way whether only a single sphere would produce the complete optical phenomenon, a $60\,\mu$m diameter glass bead on a surface-coated mirror was illuminated by the beam of a green laser. It proved to be the case that the typical interference pattern was projected in the direction of regular reflection (Fig. 5) consisting of a system of rings superimposed with horizontal fringes. This result can be regarded as justification for the restriction of our model to optical processes on one individual sphere. Further proof for the correctness of this assumption for the model is demonstrated by an image resulting from a similar experiment and published in [9], which compares well with Fig. 5.

Figure 6 illustrates the path of rays assumed in our model. A small sphere with radius r rests on a specular surface and receives light at an angle of incidence ε from a planar wave I. To simplify the model, we refrain from considering the imperfectness and inhomogeneity of an algal cell. Instead, we replace this by a perfect sphere consisting of a homogeneous material. Since it is completely symmetrical around its center and we want to explain only the far field scattered intensity pattern, we can assume that the entire scattering power of the sphere is concentrated at its center C. This assumption serves to simplify our model drastically because we only have to consider the two rays that can reach the scattering center C. These are the ray I_2, which impinges directly on it, and the ray I_1, which first hits the specular surface and afterward is reflected onto it. If the size of r is in the range of the above mentioned algae and water droplets (i.e., $3\,\mu$m to $8\,\mu$m), the dominating scattering process at C is forward scattering. Therefore, the light of ray I_2 is most intensely scattered in its initial propagation direction. Afterward, it hits the specular surface on which it is reflected. Similarly, the light of the reflected ray I_1 is most intensely scattered in the direction of propagation of the reflected ray I_1. Pairs of parallel rays that contribute to the formation of the interference pattern can be selected from both diverging bundles of rays originating from C. For further deliberations, we arbitrarily select the pair S_1, S_2 with the angle of emergence α.

Decisive for the intensity of light at the point where the rays S_1 and S_2 impinge on a screen is their

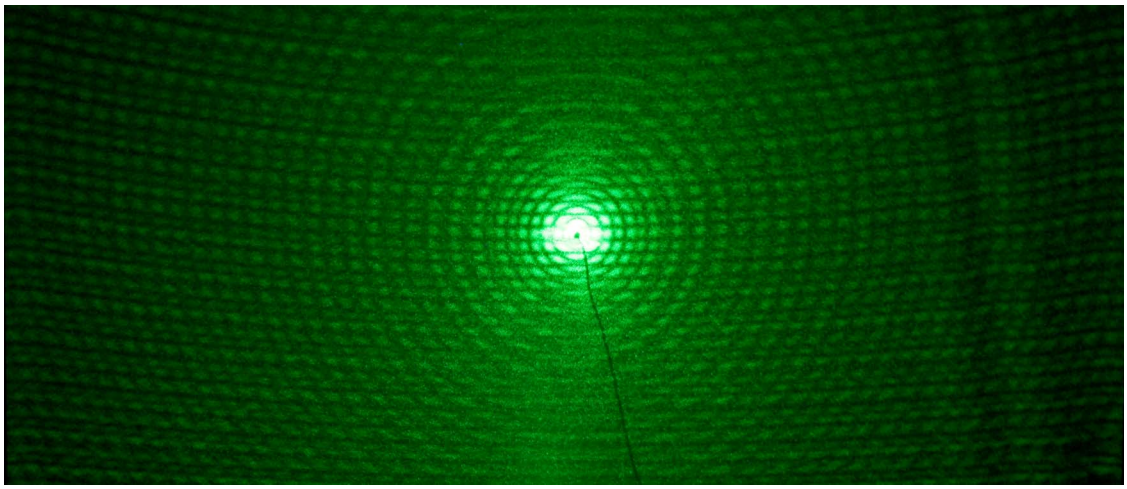

Fig. 5. (Color online) This interference pattern was projected in the direction of regular reflection with a 60 μm diameter glass bead on a surface-coated mirror illuminated by the beam of a green laser. The pattern consists of a system of rings superimposed with horizontal fringes.

optical path difference δ. A different way of representing the path of rays shown in Fig. 7 offers a clear diagram of how to compute δ. The drawing illustrates the inclusion of the "mirror world" by complementing the real sphere and the real incident rays with their virtual counterparts. Since the virtual sphere can be regarded as optically effective, together with the real sphere, it represents a bisphere. Therefore, illumination of a real bisphere with the plane wave V, whose rays V_1 and V_2 impinge on the respective centers, should produce the same interference pattern as an illuminated single sphere on a specular surface. This prediction was also confirmed experimentally. For this purpose, we placed two glass beads with a diameter of 60 μm close together on a glass slide (Fig. 8). A green laser beam passing through the slide illuminated this bisphere. The interference pattern projected forward to a screen is shown in Fig. 9, where the rings of the corona, overlapped by Quételet's fringes, are only recognizable up to the sixth order. The absence of higher order rings is probably due to a small difference in size of the two glass beads. Hence, rings of higher order were washed out by averaging. The experimental outcome, however, confirmed the optical equivalence between a single sphere placed on a specular surface and a corresponding bisphere.

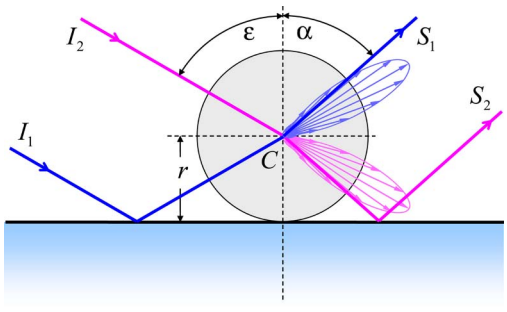

Fig. 6. (Color online) Schematic sectional view of a small sphere on a specular surface. The incident rays I_1 and I_2 are scattered at C.

In order to determine the optical path difference δ between S_1 and S_2, we refer to the geometrical situation shown in Fig. 7, where the refractive index n of the sphere has no influence because the length of the optical path to cross the respective sphere equals $2rn$ for both rays, V_1S_1 as well as V_2S_2. Derived from geometry, the optical path difference can be expressed as $\delta = 2r(\cos\alpha - \cos\varepsilon)$. According to this expression, the diffraction pattern originating from the bisphere is modulated so that maxima of order m (with $m = 1, 2, 3, \ldots$) appear at $m\lambda = 2r(\cos\alpha - \cos\varepsilon)$, provided monochromatic light with the wavelength λ is used for illumination. The identity of those maxima with the maxima of Quételet's fringes can be demonstrated by the following mental image. Let us suppose the plane within which the rays S_1 and S_2 are located is hinged to the vertical axis that combines the centers of both spheres. This allows the plane to be swiveled out of the drawing plane. Provided the angle of emergence α remains constant, then, while this plane is rotated, the rays S_1 and S_2 sweep along the surface

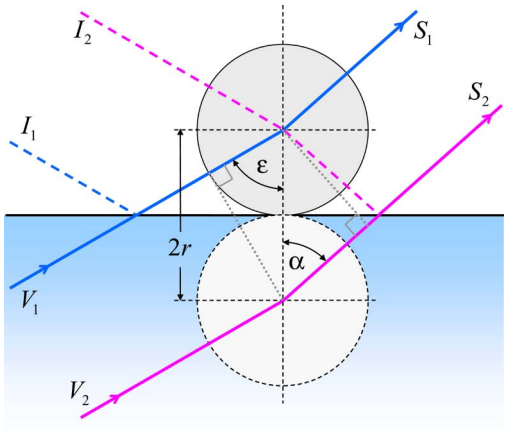

Fig. 7. (Color online) Assumed path of rays in Fig. 6, complemented by the mirror world. This figure offers a clear diagram for computation of the path difference δ.

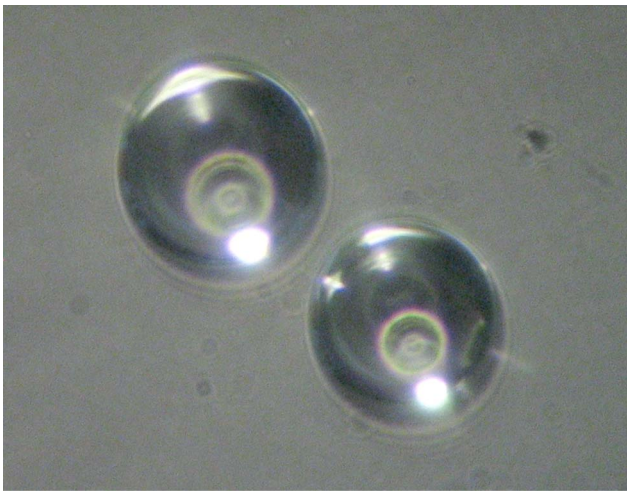

Fig. 8. (Color online) Analogous model of the optical constellation shown in Fig. 7, consisting of two 60 μm diameter glass beads on a glass slide.

of a cone. This cone can be considered as the geometrical locus where δ is constant. If the cone intersects with a planar screen, then the intersection line is a conic section. The better α fulfills the condition for the formation of maxima mentioned above, the brighter it appears on the screen.

Crucial for the location of Quételet's fringes is the distance vector between the two scattering centers of the bisphere. Since its magnitude equals $2r$ and the angles ε and α are related to its direction, all quantities needed to calculate δ depend on this. The decisive factor for the intensity of Quételet's fringes is the direction-dependent distribution of the intensity of light scattered by both scattering centers. The difference in angles between the direction of the propagation of incident light and light in a particular direction of scattering can be expressed as $\theta = \varepsilon - \alpha$. In view of this, $P(\theta)$ is a scattering function that represents the angular distribution of the relative intensity of light scattered by a single small sphere, as worked out in theory by Mie. When this scattering function is used in the following, possible optical interactions, such as mutual shading between spheres forming a bisphere, are not taken into consideration. The typical intensity pattern arising from the scattering function of a sphere (of the size range in question) is a circular corona.

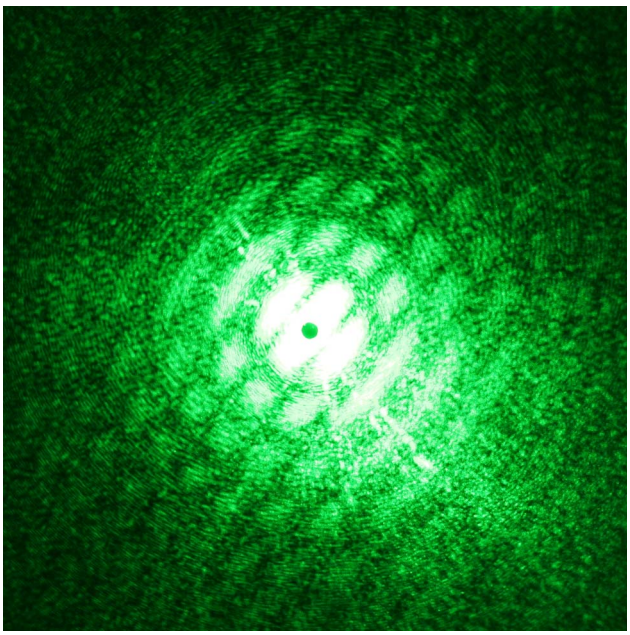

Fig. 9. (Color online) Interference pattern projected forward to a screen, with the bisphere shown in Fig. 8 illuminated by a green laser beam.

In order to obtain Quételet's fringes, other scattering objects can be used instead of small spheres. The bisphere, for example, could be replaced by two circular disks of the same diameter, while the distance vector between both scattering centers remains the same. Then, according to Babinet's principle, the diffraction pattern of a complementary double circular aperture would be identical. The scattering function $P(\theta)$ corresponding to a single aperture would then give rise to a Fraunhofer diffraction pattern. In the limit of small angles θ, an exchange of a bisphere by two complementary apertures would not affect the location of Quételet's fringes. Such an exchange, however, would be accompanied by a change of $P(\theta)$ that specifies the appearance of the diffraction pattern being modulated by Quételet's fringes. Considered from this point of view, there is a remarkable equivalence between interference fringes produced with two pinholes in Young's experiment and Quételet's fringes produced with bispheres. A more in-depth comparison between light scattering by bispheres and aperture diffraction by Young's double circular aperture is described in [10]. As stated above, the formation of interference fringes in principle demands only a real scattering object and its image formed by a plane mirror. Accordingly, the double circular aperture used in Young's experiment could be replaced by a single aperture located close to a surface-coated mirror whose plane is perpendicular to the plane of the aperture.

The classical approach to describe quantitatively the interference pattern that arises from Young's double circular aperture can be brought into the condensed expression $I(\theta) = I_0 P(\theta)\cos^2(k\delta/2)$, where $k = 2\pi/\lambda$ is the wavenumber. The expression includes the scattering function $P(\theta)$, which can be represented analytically by $P(\theta) = [2J_1(kr\sin\theta)]^2/[kr\sin\theta]^2$, where r is the radius of the aperture and J_1 is the first order Bessel function. The modulation of intensity by interference fringes (which can be considered as Quételet's fringes) can be attributed to the interference term $\cos^2(k\delta/2)$ given in the above expression. Replacing δ by the expression derived above to determine the optical path difference leads to $\cos^2(kr(\cos\alpha - \cos\varepsilon))$. Our numerical model, associated with scattering of bispheres, uses a comparable approach to compute the location of Quételet's fringes. The main difference consists of the use of a different scattering function $P(\theta)$ that is suitable

Fig. 10. (Color online) Direct view of an interference pattern on a surface-coated mirror covered with lycopodium spores and illuminated with white light.

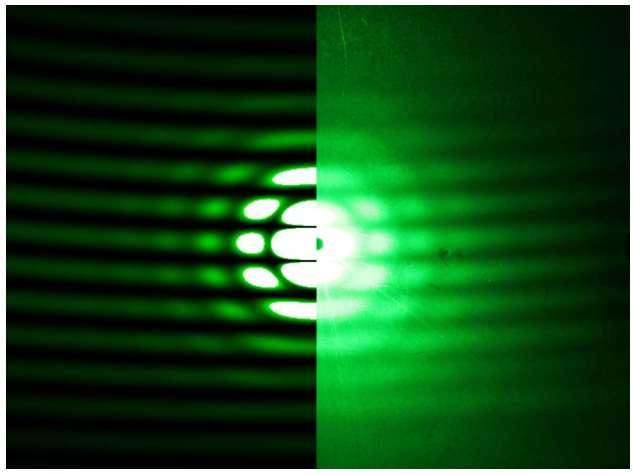

Fig. 12. (Color online) Comparison between the result of a laboratory experiment and a corresponding simulation. Right: the interference pattern was projected in the forward direction with hot water illuminated by the beam of a green laser. Left: the respective interference pattern for an ensemble of disperse spheres $\bar{r} = 8\,\mu$m ($\pm 5\%$) as calculated with our model. To obtain adequate spacing of Quételet's fringes, we also had to assume that the droplets hover $3\,\mu$m above the water.

for small spheres. For a set of scattering angles, the respective relative intensities were numerically computed using the program MiePlot, which is based on the classic BHMIE algorithm for Mie scattering from a sphere. The author of this instructive program presents its wide spectrum of applicability in [11].

Practical proof for the exchangeability of the scattering function $P(\theta)$ in our model was performed with lycopodium spores, which were strewn on a surface-coated mirror. Under suitable lighting conditions, this constellation (consisting of opaque scattering particles of almost spherical shape) also produced a corona overlapped by Quételet's fringes (Fig. 10).

The transferability of the results of our simulation model from only one bisphere to an ensemble of bispheres is limited. Our model is applicable only for an ensemble of bispheres within which the distance vector between the scattering centers of each bisphere has the same direction. If the orientations of those distance vectors were statistically distributed, the Quételet's fringes would be washed out by averaging, as described in [12]. What would remain is a pattern for randomly oriented bispheres that is quite close to the one for single spheres (with a size equal to that of the bisphere components) and that is equivalent to a corona.

Our first computations assumed an ensemble of uniformly sized small spheres. As a result, we obtained a simulated interference pattern showing high orders of interference. In contrast, our laboratory experiments with ensembles of tiny glass spheres on a surface-coated mirror (Fig. 11) or with ensembles of tiny droplets on hot water (Fig. 4) yielded far fewer orders. The conclusion to be drawn, therefore, was that the radii of the spheres deviate statistically from the median. Consequently, a phase function $P(\theta)$, calculated by MiePlot for drops disperse in size, was used in our model. Figure 12 compares the interference patterns produced by a laboratory experiment with its corresponding simulation. The right half of Fig 12 shows a photographed interference pattern that was projected onto a screen when droplets on hot water were illuminated with monochromatic light ($\lambda = 535\,$nm, $\varepsilon = 70°$). The respective interference pattern on the left half has been

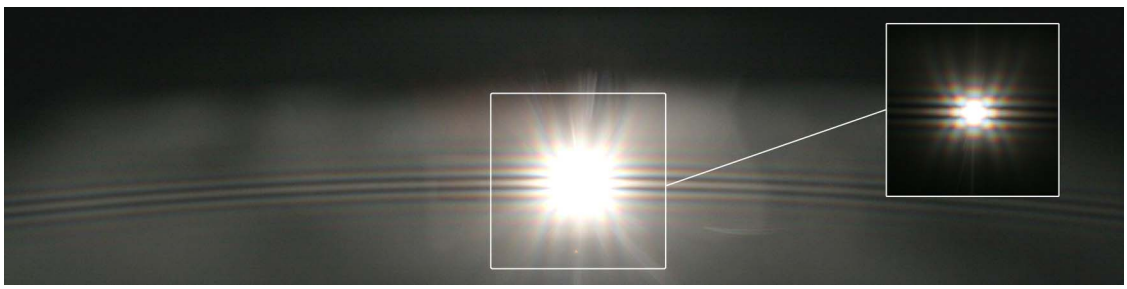

Fig. 11. (Color online) Ensemble of $60\,\mu$m diameter glass beads on a surface-coated mirror illuminated with white light. A corona overlapped by Quételet's fringes occurs around the reflection of the source of the light. (Inset: using a shorter shutter speed improved the visibility of the corona.) Both of these phenomena exhibit only the first four orders of interference.

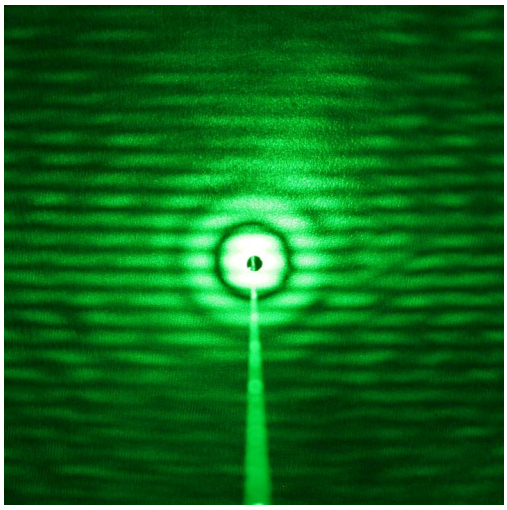

Fig. 13. (Color online) Superposition of a glory with Quételet's fringes. The interference pattern is a result of backscattering by a single 60 μm diameter glass bead on a surface-coated mirror illuminated by a green laser beam.

calculated with our model, which proceeds on the assumption of an ensemble of disperse spheres, of which the radii have a standard deviation of 5% of the median radius $\bar{r} = 8\,\mu$m. In order to determine the median radius of the droplets, we measured the angular distance of the rings of the corona in the laboratory. The value of the standard deviation of r had to be estimated. Due to our first assumption of hovering droplets in direct contact with the water surface, our computation returned an unrealistic spacing of Quételet's fringes. In order to obtain the spacing observed by computation, we had to assume additionally that the droplets hover 3 μm above the water surface. Measuring the spacing of Quételet's fringes could, therefore, be a practicable method to determine the distance between the scattering center and the mirroring surface with the aid of the interference term.

4. Concluding Remarks

A corona overlapped by Quételet's fringes can be regarded as characteristic for the optical everyday phenomena described in this paper. In order to emulate these phenomena in a laboratory, one can build an analogous model consisting of small glass spheres (or spheres made of other materials) that are placed on a surface-coated mirror. Comparably, the occurrence of the phenomenon on hot water is based on a mirroring water surface above which droplets hover closely. We therefore support the assumption made in [8] that spherical algae located just above the mirroring water surface are the cause for the occurrence of a comparable interference pattern on ponds.

Based on the model assumption that the entire scattering power of the small sphere is concentrated in its center, the location of Quételet's fringes can easily be determined by numerical simulation. This allowed us to compare our simulations with our observations. With hot water, we achieved a good match for the spacing of Quételet's fringes when we assumed that the droplets hover 3 μm above its surface. In order to achieve a good match with respect to the visible high orders of the corona, we had to assume a layer of disperse spheres whose radii have a standard deviation of 5% of the median radius $\bar{r} = 8\,\mu$m.

If one abstracts from the real scattering particles, only a layer of scattering centers, a plane parallel to a mirroring surface, remains. In this regard, there is a close connection to the optical constellation used to produce Quételet's fringes in the classical way, a process outlined in Section 1. In either case, the decisive scattering takes place at points equidistant to the mirroring surface. However, if the scattering particles used to produce Quételet's fringes in the classical way are not of uniform shape, no corona will occur.

Due to the high intensity of forward scattering by small spheres, the resulting interference patterns are easily observable, which is why our paper concentrates on these. For completeness, the fact that Quételet's fringes can arise from the much weaker backscattering should also be mentioned. As an example, Fig. 13 shows the superposition of a glory with Quételet's fringes. The interference pattern shown there was a result of backscattering by a single 60 μm diameter glass bead on a surface-coated mirror illuminated by a green laser beam.

References

1. H. J. Schlichting, "Farbkränze auf staubigen Gewässern," Phys. Unserer Zeit **35**, 86–89 (2004).
2. Isaac Newton, *Opticks*, new ed. (Prometheus, 2003). (originally published 1704)
3. K. Exner, "Ueber die Fraunhofer'schen Ringe, die Quetelet'schen Streifen und verwandte Erscheinungen," Ann. Phys. (Leipzig) **240**, 525–550 (1878).
4. W. Suhr and H. J. Schlichting, "Coloured rings produced on transparent plates," Phys. Educ. **42**, 566–571 (2007).
5. G. G. Stokes, "On the colours of thick plates," Trans. Cambridge Philos. Soc. **9**, 147–176 (1856).
6. A. J. de Witte, "Interference in scattered light," Am. J. Phys. **35**, 301–313 (1967).
7. V. J. Schaefer "Observations of an early morning cup of coffee," Am. Sci. **59**, 534–535 (1971).
8. M. Riikonen, "Optical phenomena from algal films on the water surface," Master's thesis (University of Helsinki, 2008).
9. Y. S. Kaganovskii, V. D. Freilikher, E. Kanzieper, Y. Nafcha, M. Rosenbluh, and I. M. Fuks, "Light scattering from slightly rough dielectric films," J. Opt. Soc. Am. A **16**, 331–338 (1999).
10. S. Lecler, Y. Takakura, and P. Meyrueis, "Interpretation of light scattering by a bisphere in the electrodynamic regime based on apertures interference and cavity resonance," J. Opt. A: Pure Appl. Opt. **9**, 802–810 (2007).
11. P. Laven, "Simulation of rainbows, coronas and glories by use of Mie theory," Appl. Opt. **42**, 436–444 (2003).
12. M. I. Mishchenko, D. W. Mackowski, and L. D. Travis, "Scattering of light by bispheres with touching and separated components," Appl. Opt. **34**, 4589–4599 (1995).